International Journal of Nanomedicine

Dovepress
open access to scientific and medical research

Open Access Full Text Article

ORIGINAL RESEARCH

A novel ion-exchange carrier based upon liposome-encapsulated montmorillonite for ophthalmic delivery of betaxolol hydrochloride

This article was published in the following Dove Press journal:
International Journal of Nanomedicine
2 March 2017
Number of times this article has been viewed

Yi Huang[1]
Qi Tao[2]
Dongzhi Hou[1]
Sheng Hu[1]
Shuangyan Tian[1]
Yanzhong Chen[3]
Ruyi Gui[1]
Lingling Yang[4]
Yao Wang[5]

[1]College of Pharmacy, Guangdong Pharmaceutical University, [2]Key Laboratory of Mineralogy and Metallogeny, Chinese Academy of Sciences, Guangdong Provincial Key Laboratory of Mineral Physics and Materials, [3]Guangdong Provincial Key Laboratory of Advanced Drug Delivery Systems, Guangdong Pharmaceutical University, Guangzhou, [4]State Key Laboratory Cultivation Base, Shandong Provincial Key Laboratory of Ophthalmology, Shandong Eye Institute, Shandong Academy of Medical Sciences, [5]Qingdao Eye Hospital, Shandong Eye Institute, Shandong Academy of Medical Sciences, Qingdao, China

Abstract: As a novel ion-exchange carrier with high surface area and excellent exchangeability, montmorillonite (Mt) was intercalated with betaxolol hydrochloride (BH) to form a nanocomposite and then encapsulated by liposomes (Mt-BH-LPs) for an ophthalmic drug-delivery system. The Mt-BH and Mt-BH-LPs were prepared by an acidification process and ethanol injection combined with ammonium sulfate gradient methods. The successful formation of Mt-BH and Mt-BH-LPs was verified by thermogravimetric analysis, X-ray diffraction, Fourier-transform infrared spectra, and transmission electron microscopy. Mt-BH-LPs possessed the favorable physical characteristics of encapsulation efficiency, drug loading, mean particle size, and ζ-potential. In vitro release studies indicated Mt-BH-LPs effectively maintained a relatively sustained slow release. Immortalized human corneal epithelial cell cytotoxicity, in vivo rabbit eye-irritation tests, and chorioallantoic membrane–trypan blue staining all revealed that Mt-BH-LPs had no obvious irritation on ocular tissues. A new in vitro tear-turnover model, including inserts containing human corneal epithelial cells, was designed to evaluate the precorneal retention time of Mt-BH-LPs. The results showed that Mt-BH-LPs maintained a certain BH concentration in tear fluid for a longer period than the BH solution. In vivo precorneal retention studies also indicated Mt-BH-LPs prolonged drug retention on the ocular surface more than the BH solution. Furthermore, pharmacodynamic studies showed that Mt-BH-LPs had a prolonged effect on decreasing intraocular optical pressure in rabbits. Our results demonstrated that Mt-BH-LPs have potential as an ophthalmic delivery system.

Keywords: liposome, montmorillonite, irritation, precorneal retention time, intraocular optical pressure

Introduction

Glaucoma is the most common cause of ocular disease, and is attributed to a rise of intraocular pressure (IOP) that finally results in the loss of vision.[1,2] During the past few decades, great efforts have been made to improve the effects of conventional ophthalmic dosage forms to eliminate this ocular disease, but the drawback of blurred vision has mainly hindered their wide acceptance.[3] Betaxolol hydrochloride (BH) has been employed for the treatment of this problem, due to its superior ability of selective β_1-receptor and calcium-channel blocking.[4] These characteristics can effectively suppress aqueous humor generation and increase its effusion, resulting in a reduction in IOP and inhibition of disease progression. However, application of BH is limited by its extremely low bioavailability and some side effects. The low bioavailability of BH is mainly due to the poor permeability of the cornea to drugs. Therefore, a novel local ocular delivery system for BH needs to develop to improve preocular retention and drug absorption.[5]

Correspondence: Dongzhi Hou
College of Pharmacy, Guangdong Pharmaceutical University, Middle Ring Road East, Higher Education Mega Center, Panyu Qu, Guangzhou, Guangdong 510006, China
Tel/fax +86 20 3935 2117
Email houdongzhi406@163.com

submit your manuscript | www.dovepress.com
Dovepress
http://dx.doi.org/10.2147/IJN.S122747

In recent years, various ophthalmic drug-delivery systems have been developed for ocular carriers, including liposomes (LPs),[6–8] nanoparticles,[9,10] microspheres,[11,12] nanostructured lipid carriers,[13,14] in situ gels,[15,16] and contact lenses.[17] Among these, LPs have proved to be a promising formulation for ocular drug transport in the last decade, because they include enclosed vesicles and bilayer structures. These structures have many favorable features, including good biocompatibility, non-immunogenicity and sustained release.[18,19] Furthermore, LPs have suitable particle size (PS) and ζ-potential (ZP), which can improve precorneal residence ability and drug uptake.[20] Therefore, LPs may be a good candidate for enhancing the ocular bioavailability of topically administered drugs.

Montmorillonite (Mt) is a novel ion-exchange drug carrier with high surface area and excellent exchangeability.[21,22] In recent years, Mt intercalated by drug molecules with different structures has attracted great interest from researchers, as the different structures have exhibited improved drug release properties. Zheng et al studied the intercalation of ibuprofen molecules into an Mt interlayer as a sustained-release drug carrier.[23] Fejér et al investigated the intercalation and release behavior of promethazine chloride and buformin hydrochloride from Mt.[24] Nunes et al reported the loading and delivery of sertraline using Mt K10.[25] Our research has also shown that solid lipid nanoparticles[22] and chitosan nanoparticles[26] intercalated with Mt–drug nanocomposites to form nanocarriers can serve as promising ocular drug-delivery systems.

In this study, for the first time, BH was intercalated with Mt and then encapsulated by LPs to construct a novel nanocarrier of Mt-BH-LPs, which were prepared by acidification of Mt and ethanol injection combined with ammonium sulfate gradient methods, respectively. The microscopic characteristics of Mt-BH-LPs were measured by Fourier-transform infrared spectroscopy (FTIR), thermogravimetric analysis (TGA), X-ray diffraction (XRD), and transmission electron microscopy (TEM). Pharmaceutical evaluation of Mt-BH-LPs was conducted subsequently, including encapsulation efficiency (EE), drug-loading (DL) rate, PS, ZP, and in vitro drug-release behavior. Three different tests were applied to evaluate irritation of the Mt-BH-LP drug-delivery system, including immortalized human cornea epithelial cell (iHCEC) cytotoxicity test, in vivo rabbit eye-irritation test, and chorioallantoic membrane–trypan blue staining (CAM-TBS). Finally, the pharmacokinetics and pharmacodynamics of Mt-BH-LPs were also investigated, including in vitro and in vivo precorneal retention and the effect of these ophthalmic formulations on IOP.

Materials and methods

Materials

Mt was obtained from Aladdin Biochemical Technology (Shanghai, China). BH was purchased from Hao Industrial (Jinan, China). Phosphatidylcholine (PC) was obtained from Taiwei Pharmaceutical (Shanghai, China). MTT and all components of buffer solutions were from Sigma-Aldrich (St Louis, MO, USA). All other chemical reagents used in the study were of high-performance liquid chromatography (HPLC) or analytical grade.

Preparation of Mt-BH and Mt-BH-LPs

Mt-BH was prepared based on acidification of Mt under different reaction conditions.[22,27,28] BH solution (100 mL 3 mg·mL^{-1}) and 100 mg acid-Mt were mixed in a beaker. After the dispersion's pH had been adjusted to 4, the mixture was left static for adsorption to occur in a 50°C water bath for 6 hours. The solid and liquid phases were separated by centrifugation and the solid Mt-BH dried and then stored for further treatment. Mt-BH-LPs were prepared by ethanol injection combined with an ammonium sulfate gradient.[29,30] Briefly, 225 mg PC, 25 mg cholesterol, and octadecylamine were placed in 5 mL ethanol as the oil phase at 60°C. Mt-BH was added into the oil phase and ultrasonified for 10 minutes. Then, the mixture was slowly injected into the 10 mL 0.15 mol·L^{-1} ammonium sulfate and stirred for 30 minutes. After further evaporation of the organic solvents, the resulting residue was added to BH to form Mt-BH-LPs spontaneously. BH-LPs were prepared with the same steps, but without the addition of Mt-BH. The obtained BH-LPs and Mt-BH-LPs were stored at 4°C. The preparation process of Mt-BH-LPs is shown in Figure 1.

Entrapment efficiency and drug-loading rate

EE and DL of Mt-BH-LPs were investigated by dynamic dialysis.[31] The free BH was separated by dialysis using a dialysis bag with molecular weight of 12–14 kDa. Mt-BH-LP dispersions (5 mL) were transferred into the dialysis bags, immersed in 100 mL solvent medium of normal saline, and then stirred at 120 rpm at 34°C. The drug concentration attained balance. The BH concentration in the release medium was quantified with HPLC. Acetonitrile–trimethylamine (30:70, v:v) with pH 3 was used as the mobile phase at a

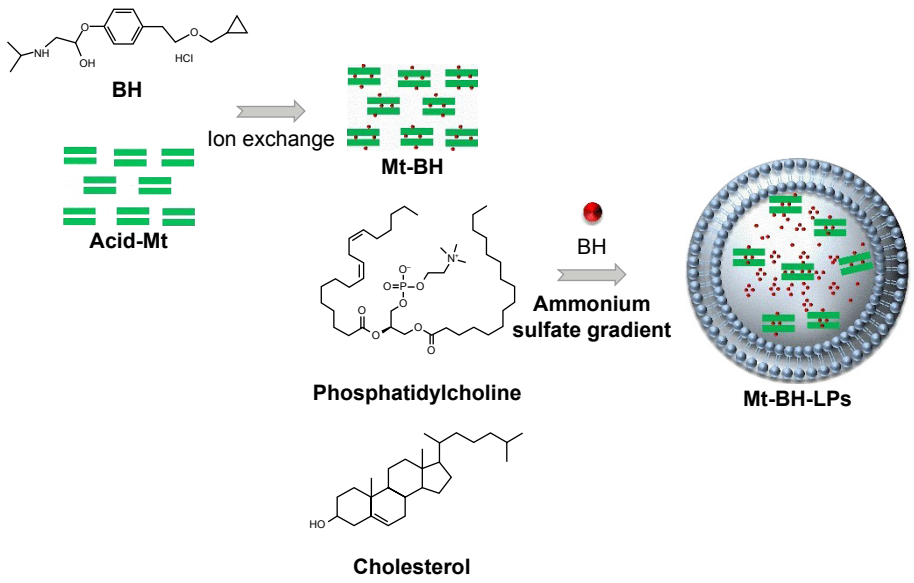

Figure 1 Schematic of the preparation process of Mt-BH-LPs.
Abbreviations: Mt-BH-LPs, montmorillonite–betaxolol hydrochloride liposomes; BH, betaxolol hydrochloride; Mt, montmorillonite.

flow rate of 1 mL·min^{-1}. The determined wavelength, column temperature, and injection volume were 275 nm, 25°C, and 20 µL, respectively. EE and DL of Mt-BH-LPs were calculated according to the following equations:

$$EE = \frac{C_0 - C}{C_0} \times 100\% \quad (1)$$

$$DL = \frac{EE \times m_{BH}}{m_{Mt-BH-LP}} \times 100\% \quad (2)$$

where, C_0, C, m_{BH} and $m_{Mt-BH-LP}$ are the BH concentration (mg·mL^{-1}) of Mt-BH-LPs without dialysis treatment, BH concentration of Mt-BH-LPs in solvent medium after dialysis treatment, dosage of BH, and mass of Mt-BH-LPs, respectively.

Characteristics

A Vertex 70 FTIR spectrometer was used to collect the spectrograms. The range, resolution, and scan times were 400–4,000 cm^{-1}, 4 cm^{-1}, and 64, respectively. TGA was measured by a Netzsch STA 409 PC/PG, and heating rate and nitrogen flow were 10°C·min^{-1} and 60 cm^3·min^{-1}, respectively. XRD patterns were determined using a Bruker D8 advance diffractometer (CuKα radiation) from 3° to 70°, and the scan rate, generator voltage, and generator current were 3°·min^{-1}, 40 kV, and 40 mA, respectively. The morphology of the Mt-BH-LPs was investigated by TEM (Tecnai 10; Philips, Amsterdam, the Netherlands) at an acceleration voltage of 115 kV. PS and ZP of the LPs were measured by dynamic light scattering and electrophoretic light scattering, respectively, both using a Beckman apparatus.

Stability studies

Mt-BH-LPs (1 mL 2.8 mg·mL^{-1}) were mixed with 10, 50, and 100 mL saline, simulated tear fluid (STF), and phosphate-buffered saline, respectively. Stability studies were conducted at 34°C without light and performed in triplicate. Changes in appearance of the samples were observed, including the color, turbidity, and precipitation. The PSs of the sample were also measured at predetermined time intervals.

In vitro release studies

The in vitro release rate of BH from Mt-BH-LPs was investigated according to the dialysis method. Mt-BH-LP (5 mL) dispersions were placed in a dialysis bag and then immersed in 100 mL release medium of STF at 34°C at 120 rpm. Briefly, 6.78 g NaCl, 2.18 g $NaHCO_3$, 0.084 g $CaCl_2 \cdot 2H_2O$, and 1.38 g KCl were dissolved in 1,000 mL deionized water to serve as STF. At predetermined time intervals, 5 mL of the release medium was withdrawn and immediately replaced with an equal amount of fresh release medium. The BH content in the release medium was determined by HPLC. Each experiment was repeated five times. The data of in vitro release studies were fitted to several drug-releasing models to determine the mechanism of drug release from the Mt-BH-LPs.

Irritation evaluation

In vitro cytotoxicity

iHCECs were cultured in Dulbecco's Modified Eagle's Medium DMEM/F12, along with 10% (v/v) fetal bovine serum (FBS), 0.1 mg·mL^{-1} streptomycin and 1,000 IU·mL^{-1} penicillin in a 37°C atmosphere containing 5% CO_2. In vitro cytotoxicity of Mt-BH-LPs was evaluated according to MTT assay, which is based on the mitochondrial conversion of the tetrazolium salt MTT.[32] Approximately 10^4 cells/cm^2 were seeded in 96-well plates and cultured for 24 hours. The culture medium was removed, and then various samples (2.8 mg·mL^{-1}) of different volumes (10, 20, 30, 50, 80, and 100 µL) with different dissolving times (0.5, 2, and 4 hours) in Dulbecco's Modified Eagle's Medium/F12 were added to the cells (100 µL per well). After 24 hours' exposure, the culture medium was removed and the cell substrate washed with phosphate-buffered saline, and then 180 µL of fresh medium and 20 µL of MTT (5 mg·mL^{-1}) were added to each well for 4 hours' treatment. At the end of the assay, the obtained formazan granules were dissolved in dimethyl sulfoxide. Cell viability was measured by spectrophotometry at 490 nm by the formula:

$$\text{Cell viability}\,\% = \frac{A_1}{A_0} \times 100\% \qquad (3)$$

where A_1 and A_0 are absorbance of the test and control group, respectively.

In vivo rabbit eye-irritation test

All animal experiments complied with the requirements of the National Act on Experimental Animals (China) and were approved by the animal ethics committee of Southern Medical University. Animals used for all experiments were the same batch number weighing 2–2.5 kg, without any signs of inflammation or gross ocular abnormality (eg, cataract, glaucoma). Twelve healthy New Zealand White rabbits were chosen for the single-dosage ocular irritation test and divided into four groups. The left eyes of every group received 50 µL normal saline as blank controls, and the right eyes were administered 50 µL sample as the test group. The eyes were examined at 1, 2, 4, 24, 48, and 72 hours after administration, and irritation was evaluated by Draize eye-test guidelines.[33] The long-term ocular irritation tests were the same as single-dosage ocular irritation tests, except administration was continued to 7 days. After irritation tests, the rabbits were killed by air injection. Eyeballs were excised and fixed by 10% formalin, and after staining with hematoxylin and eosin, histopathology of corneas and conjunctiva were observed by microscope.

Chorioallantoic membrane–trypan blue staining assay

Briefly, hen's eggs were incubated for 9 days and a portion of the egg shell above the air space removed, exposing the CAM. A 300 µL sample was applied to the CAM (defective eggs were discarded) and remained in contact for 5 minutes. Then, the sample was washed by normal saline and 0.5 mL TB solution (1 mg·mL^{-1}) was added to the CAM for 1 minute. Finally, the dyed CAM was excised and the adsorbed TB extracted with 1 mL formamide for 24 hours. The extract was determined by UV at 611 nm in quintuplicate. Normal saline and 0.1 mol·L^{-1} NaOH were used as negative and positive control groups, respectively. The absorbed amount of TB was proportional to the irritation.

Precorneal retention of Mt-BH-LPs

In vitro precorneal retention of Mt-BH-LPs

iHCEC layers were used as a model. Before cultivation, an ethanolic solution of type I rat-tail collagen (1.5 mg·mL^{-1}) that had been acidulated with acetic acid was cast in a Transwell, and then an aqueous solution of fibronectin (10 µg·mL^{-1}) was flowed onto the collagen-coated filter. After removal of the fibronectin solution, the iHCECs dispersed in the culture medium were seeded onto the filter, and when the iHCECs became confluent, cell differentiation and multilayered growth of the epithelium was induced by lifting the construct to the air–liquid interface to have a varying period of submerged cultivation. Precorneal retention time of Mt-BH-LPs versus solution was evaluated by using an in vitro tear-turnover apparatus (Figure 2) and the inserts in which corneal tissue had been cultured as a turnover chamber. Then the inserts were placed in a thermostating bath at 34°C to maintain the temperature of the human TF. The in- and outflow of tears in the chamber were controlled by a peristaltic pump. Each experiment started by transferring 30 µL of the sample (2.8 mg·mL^{-1}) in the turnover chamber

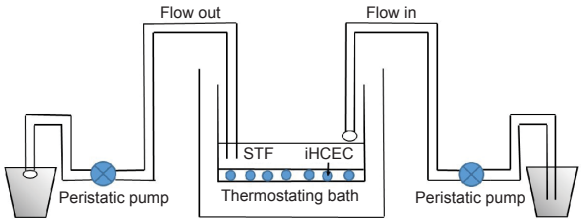

Figure 2 Schematic diagram of the in vitro tear-turnover apparatus.
Notes: The model incorporated an insert containing cultured corneal tissue as a turnover chamber; the external basal side of the insert was sealed to avoid a downward diffusion of material. The system was temperature-controlled at human tear-film temperature (34°C). Constant in- and outflow of simulated tears in the chamber were controlled by peristaltic pumps.
Abbreviations: STF, simulated tear fluid; iHCEC, immortalized human corneal epithelial cell.

prefilled with 270 µL of STF. Every 10 minutes, 500 µL of collected solution and precorneal retention time was determined by HPLC with fluorescence detection.

In vivo precorneal retention of Mt-BH-LPs

Precorneal retention ability of Mt-BH-LPs was evaluated by using a tear-elimination method.[34] Briefly, six healthy New Zealand White rabbits were chosen and divided into BH-solution and Mt-BH-LP groups. Samples (50 µL) were dropped into conjunctival sacs of rabbits, and then the eyes were closed for 1 minute. At predetermined time intervals, an 8×8 cm paper was placed in the conjunctival sac to absorb tears for 1 minute. The Δm of paper was regarded as the weight of absorbed tears. Each sample was dried and extracted by 200 µL methanol, vortexed for 5 minutes, and centrifuged at 15,000 rpm for 15 minutes. The supernatant was determined by HPLC and BH concentration in tears using the formula:

$$C_0 = \frac{C \times V_0 \times \rho}{\Delta m} \quad (4)$$

where C_0 is the drug concentration in tears, C the drug concentration in methanol, ρ the density of tears (ρ=1), and Δm the weight of tears.

Pharmacodynamic studies

New Zealand albino rabbits with weight 2–2.5 kg were used for in vivo pharmacodynamic studies. Rabbits were kept in a dark room for 5 hours before the experiment.[35] IOP was measured by an indentation tonometer (YZ7A; Suzhou Visual Technology Co Ltd, Suzhou, China) under surface anesthesia (0.2% lidocaine hydrochloride). These six rabbits were divided into two groups: one instilled with 50 µL Mt-BH-LPs into the left eye, and the other instilled with equal BH solution into the left eye. To avoid experimental bias, 50 µL normal saline was placed in the conjunctival sac of the right eye (control) and kept open for about 1 minute to prevent the eyedrops from overflowing. IOP of all eyes was measured eight times at predetermined time intervals (0, 0.5, 1, 2, 3, 4, 5, and 6 hours). Each measurement obtained three readings.

Results and discussion

Pharmaceutical evaluation

There was no increase in drug concentration for up to 2 hours, indicating that the free drugs dialyzed out completely and drug concentration attained balance at 2 hours (Figure 3). EE and

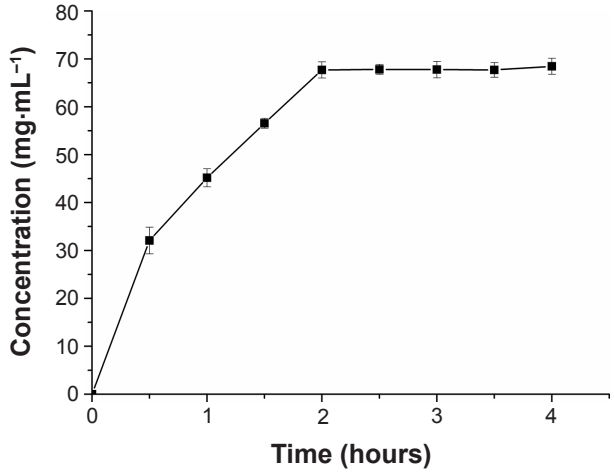

Figure 3 Time to dialysis equilibrium of Mt-BH-LPs.
Abbreviation: Mt-BH-LPs, montmorillonite–betaxolol hydrochloride liposomes.

DL of Mt-BH-LPs were 75.85%±2.15% and 11.41%±0.29% (n=3), respectively. Ethanol injection combined with the ammonium sulfate gradient was efficient and reproducible. PS is of great importance in affecting the cellular uptake of topically administered drugs. The PS limit for human-eye tolerance is about 10 µm, and thus the carrier with smaller PS shows better ability to cross the biobarrier and has better patient compliance.[36] ZP is another key factor in controlling the stability of ophthalmic drug-delivery systems. As shown in Figure 4A, PS, ZP, and polymer-dispersion index values for BH-LPs without Mt incorporation were 166.4±1.89 nm, 19.33±0.41 mV, and 0.155±0.019, respectively. After the loading of Mt into the BH-LPs, mean PS, ZP and PDI values for Mt-BH-LPs were 218±22.32 nm, 17.03±0.25 mV, and 0.191±0.064, respectively (Figure 4B). This indicated that the loading of Mt into the BH-LPs had little effect on the parameters of PS and ZP, which was beneficial for its application in an ocular drug-delivery system. Stability studies showed that no significant alteration in appearance or PS was observed.

The morphology of the Mt-BH-LPs was observed through TEM graphs (Figure 5). BH-LPs were uniformly dark solid spheres with an approximate diameter of 130 nm (Figure 5B), which was consistent with the value estimated by dynamic light-scattering analysis. On the contrary, the Mt-BH-LPs exhibited a clear double-layer vesicle shape with a slightly increasing diameter of about 180 nm after encapsulation of Mt-BH by LPs (Figure 5D). The formation of the double-layer vesicle resulted from the aggregation of LPs.

The characteristic 2θ peaks (d_{001}) of acid-Mt and Mt-BH were 5.5° and 4.8°, with corresponding basal spacing of 1.54 nm and 1.93 nm, respectively (Figure 6). The increase in d-value indicated that BH molecules had been intercalated

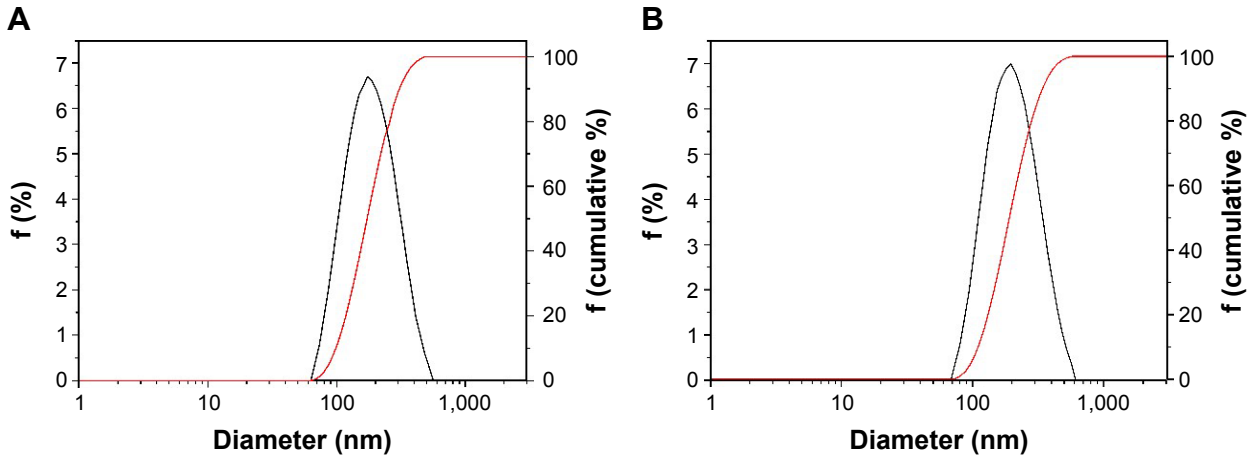

Figure 4 Particle-size distribution of (**A**) BH-LPs and (**B**) Mt-BH-LPs.
Note: The red line indicates cumulative distribution. The black line inidates the percentage of the particle size. f, differential intensity.
Abbreviation: Mt-BH-LPs, montmorillonite–betaxolol hydrochloride liposomes.

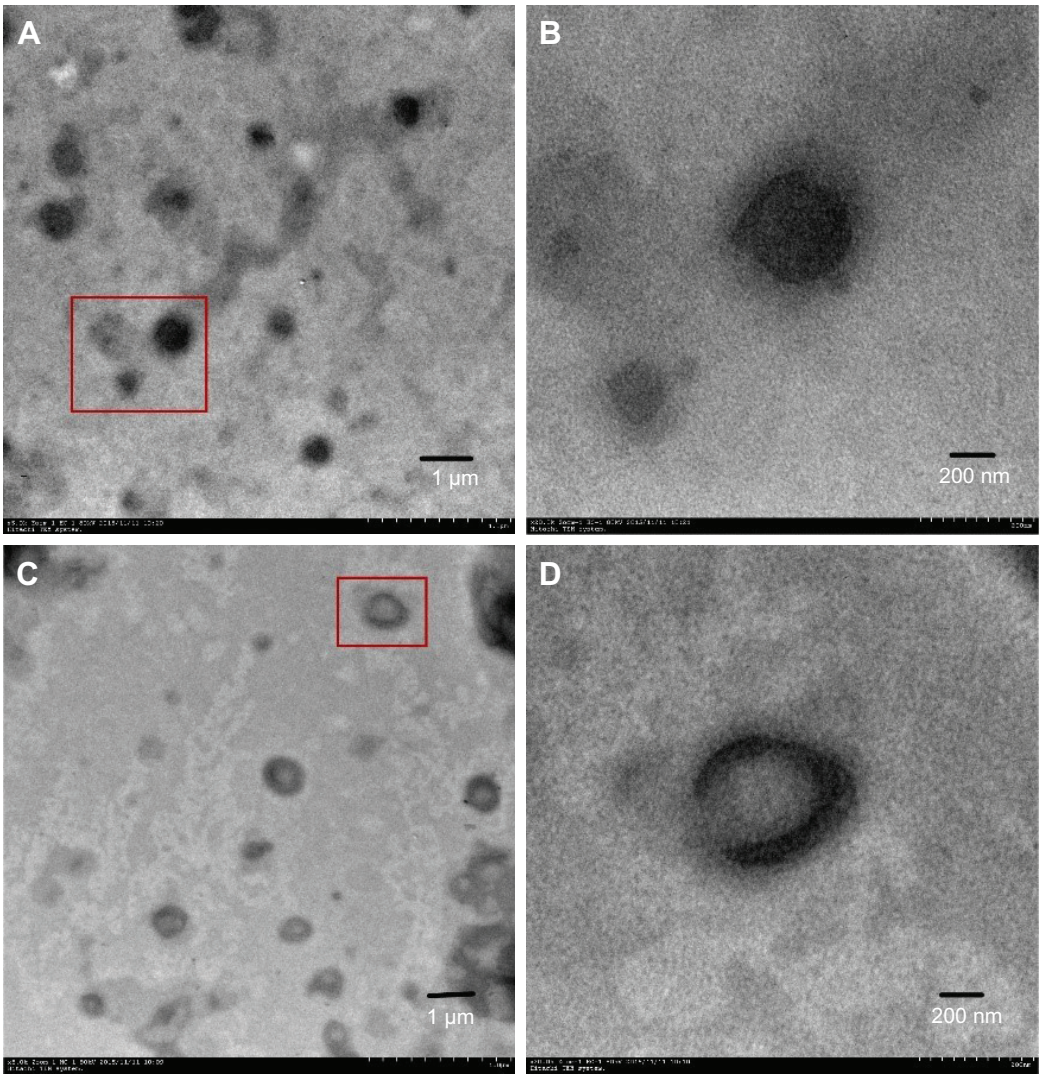

Figure 5 TEM images of (**A**, **B**) BH-LPs and (**C**, **D**) Mt-BH-LPs.
Note: (**B** and **D**) show magnification of red squares in (**A** and **C**), respectively.
Abbreviations: TEM, transmission electron microscopy; Mt-BH-LPs, montmorillonite–betaxolol hydrochloride liposomes.

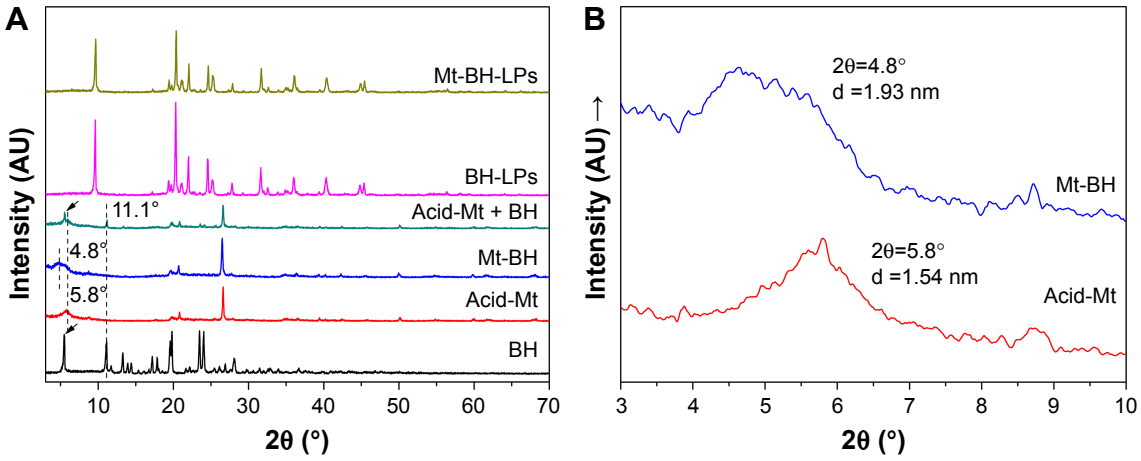

Figure 6 (**A**) XRD patterns of BH, acid-Mt, Mt-BH, acid-Mt + BH BH-LPs, and Mt-BH-LPs; (**B**) enlarged XRD patterns of acid-Mt and Mt-BH.
Abbreviations: XRD, X-ray diffraction; Mt-BH-LPs, montmorillonite–betaxolol hydrochloride liposomes; BH, betaxolol hydrochloride; Mt, montmorillonite.

into the Mt-interlayer space.[37] Surprisingly, when the acid-Mt and BH were simply mixed, the mixture showed the characteristic peaks belonged only to acid-Mt or BH, without appearance of any new peaks. This implied that the physical mixture processes did not change the lamellar spacing of the hybrid. Interestingly, the characteristic peaks of acid-Mt and Mt-BH disappeared in the Mt-BH-LP curve, due to the aggregation of chain alignment in the LPs after cross-linking, which demonstrated the Mt-BH-LPs were successfully formed.[38]

TGA and differential scanning calorimetry curves were used to explain the new chemical bonding of these hybrids further.[39,40] BH showed a sharp weight loss (about 95 wt%) at 240°C–450°C, because of its total decomposition (Figure 7). Acid-Mt showed a slight weight loss (about 8 wt%) at 120°C, due to the evaporation of adsorbed water. Compared with acid-Mt, Mt-BH possessed a slight weight loss (about 9 wt%) at 270°C–500°C, corresponding to the decomposition of the BH, which suggested BH was successfully intercalated into the Mt-interlayer space.[41] Mt-BH-LPs and BH-LPs both displayed obvious weight loss (about 67 wt%) at 170°C–600°C, due to the decomposition of LPs.[42] Furthermore, compared with BH-LPs, Mt-BH-LPs exhibited a characteristic weight loss (about 5 wt%) at 700°C–1,000°C, corresponding to the structural damage of Mt, indicating Mt-BH was successfully encapsulated by LPs.[43]

FTIR spectra of acid-Mt, BH, Mt-BH, and Mt-BH-LPs are presented in Figure 8. Absorptions at 3,431, 1,081, and 1,041 cm^{-1} belonged to –OH, Si–O, and in-plane stretching vibrations of Mt, respectively.[44] In the spectra of pure BH, absorption at 3,280, 1,612, and 1,512 cm^{-1} were ascribed to aromatic ring C–H and alkyl chain C–H stretching and

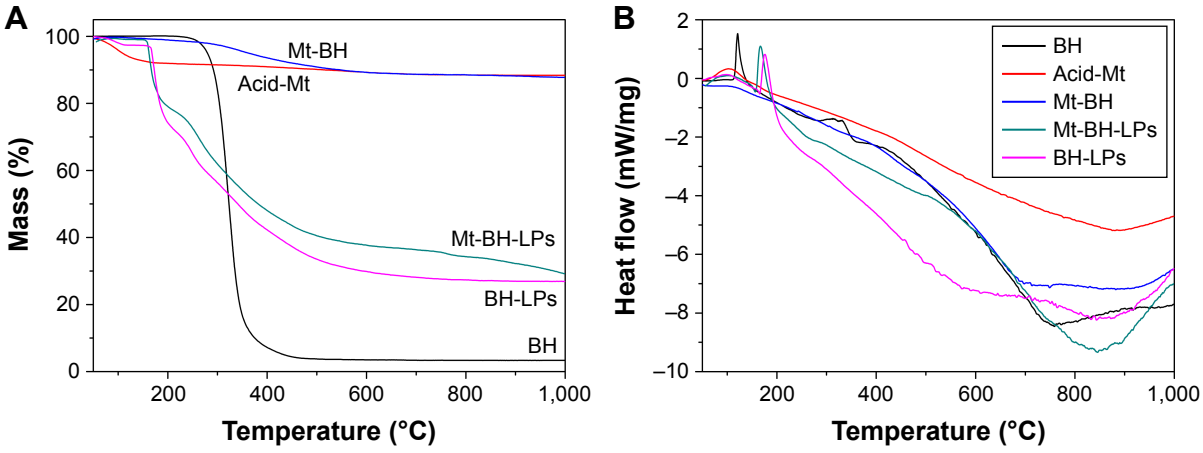

Figure 7 (**A**) TGA and (**B**) DSC pattern of BH, acid-Mt, Mt-BH, BH-LPs, and Mt-BH-LPs.
Abbreviations: TGA, thermogravimetric analysis; DSC, differential scanning calorimetry; Mt-BH-LPs, montmorillonite–betaxolol hydrochloride liposomes; BH, betaxolol hydrochloride; Mt, montmorillonite.

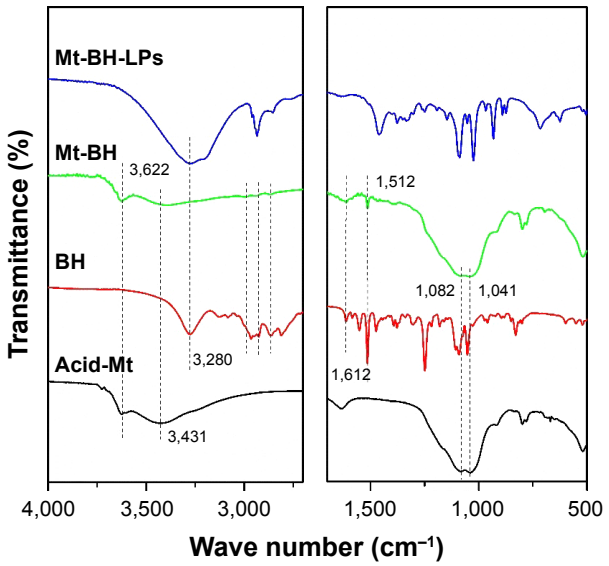

Figure 8 FTIR spectra of acid-Mt, BH, Mt-BH, and Mt-BH-LPs.
Abbreviations: FTIR, Fourier-transform infrared; Mt-BH-LPs, montmorillonite–betaxolol hydrochloride liposomes; BH, betaxolol hydrochloride; Mt, montmorillonite.

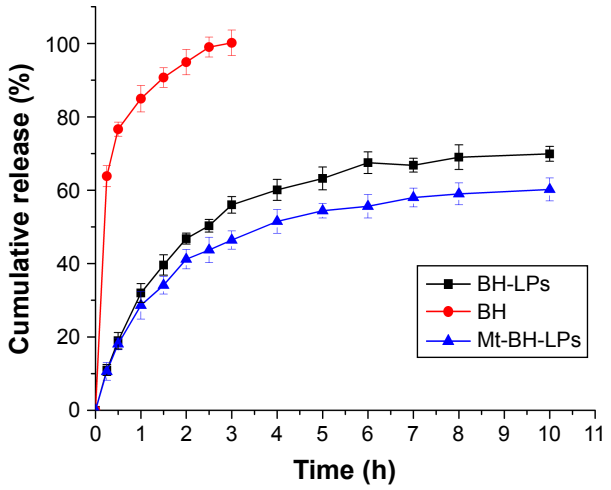

Figure 9 In vitro release curves of BH solution, BH-LPs, and Mt-BH-LPs.
Abbreviations: Mt-BH-LPs, montmorillonite–betaxolol hydrochloride liposomes; BH, betaxolol hydrochloride.

deformation vibrations. After the intercalation of BH into the Mt-interlayer space, characteristic bands (3,280 and 2,900–3,100 cm^{-1}) of BH disappeared in the spectrum of Mt-BH, which indicated that BH molecules interacted strongly with the Mt.[45] Furthermore, Mt-BH-LPs showed a broad peak around 3,100–3,500 cm^{-1} with the disappearance of characteristic bands (3,622 cm^{-1}), due to the aggregation of LPs.[46] All these variations demonstrated that Mt-BH was successfully incorporated into the LP interlayer.

In vitro release studies

To evaluate release properties of Mt-BH-LPs, in vitro release experiments were performed and compared with BH-LPs and BH solution (Figure 9). It was found that approximately 100% of BH rapidly released within 2.5 hours from the BH sample, which suggested that BH can freely diffuse through the dialysis membrane. Compared with the BH solution, BH-LPs exhibited a release of 50.3% in the initial 2.5 hours, which led to 69.9% release within 10 hours. The initial burst release of BH from BH-LPs was responsible for the adsorption of BH onto the surface of LPs. Furthermore, for Mt-BH-LPs, a slower release of only 43.7% was observed in the initial 2.5 hours compared with BH-LPs, followed by a phase of sustained release at a much slower release rate. The slower release rate of BH from Mt-BH-LPs could be ascribed to the intercalation of BH into the Mt-interlayer space. In addition, the characteristic of ion-exchange reactions and the existence of electrostatic interactions between the intercalated drug and the alkali metal ions of the buffer were responsible for a relatively sustained slow release.[47]

The drug release from simulation models showed that the in vitro drug-release profiles of Mt-BH-LPs were consistent with both the Weibull equation (r=0.9988) and the first-order kinetics equation (r=0.9913). These indicated that BH release was controlled by diffusion, as well as matrix-erosion mechanisms from Mt-BH-LPs at a suitable rate.[48]

Irritation evaluations

In vitro cytotoxicity

The viability of iHCECs after exposure to Betoptic, BH solution, blank LPs and Mt-BH-LPs in different amounts for 0.5, 2, and 4 hours is shown in Figure 10. These results showed that the cytotoxicity of each sample for cells was amount-dependent. As shown in Figure 10A, cell viability with Betoptic was the lowest among the samples. In general, cell viability was under 60% when the administration volume of Betoptic was only 10 µL. Cell viability fell sharply below 20% when the administration volume was over 20 µL. The high cytotoxicity of Betoptic might be due to its greater viscidity and electropositivity. On the contrary, the viability of iHCECs treated with 10, 20, and 30 µL of BH, blank LPs, and Mt-BH-LPs, respectively, was very high (>70%), and no obvious difference in cell survival was observed among these samples. Although viability values showed a significant decrease when the amount exceeded 100 µL, blank LP and Mt-BH-LP exposure showed higher viability for iHCECs compared with BH. This may be explained by the fact that Mt-BH-LPs can protect the cells from damage by BH (raw drug). Figure 11 shows the toxicity of Betoptic, BH, blank LPs, and Mt-BH-LPs on iHCECs at each amount

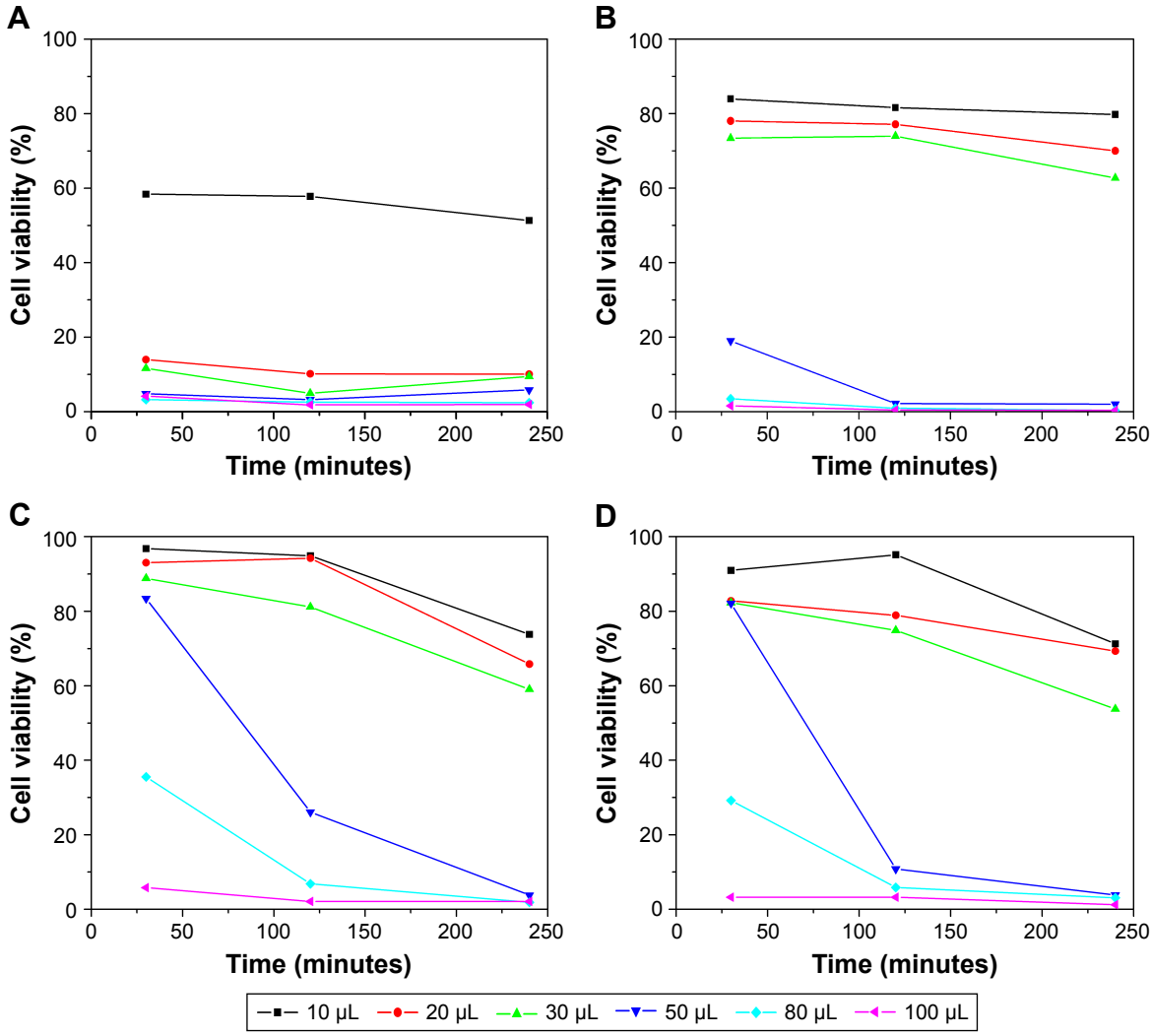

Figure 10 Cell viability of (**A**) Betoptic, (**B**) BH solution, (**C**) blank LPs, and (**D**) Mt-BH-LPs at different exposure times and amounts.
Abbreviations: Mt-BH-LPs, montmorillonite–betaxolol hydrochloride liposomes; BH, betaxolol hydrochloride.

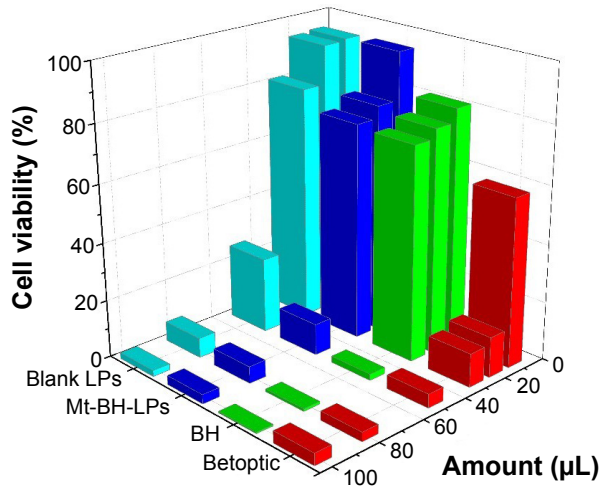

Figure 11 Viability of iHCECs with differing amounts of Betoptic, BH solution, blank LPs, and Mt-BH-LPs exposure for 2 hours.
Abbreviations: iHCECs, immortalized human corneal epithelial cells; Mt-BH-LPs, montmorillonite–betaxolol hydrochloride liposomes; BH, betaxolol hydrochloride.

(10, 20, 30, 50, 80, 100 μL) for 2 hours was Betoptic > BH > Mt-BH-LPs > blank LPs. From these results, it is clear that Mt-BH-LPs can effectively maintain superior cell viability within an appropriate range.

In vivo rabbit eye-irritation test

The ocular irritation of the BH and Mt-BH-LP formulations was estimated by the Draize method, with normal saline and Betoptic formulations as a control experiment. Cornea and iris scores for all formulations were all zero (Table 1). Though eyes showed conjunctival congestion for the BH and Mt-BH-LP formulations, there were no significant differences compared with normal saline and Betoptic. This conjunctival congestion was responsible for the sensitivity of conjunctiva to exogenous compounds. Total scores were 0–3 for all formulations in single dosages or long-term eye-irritation experiments.

Table 1 Draize test scores

	Normal saline		Betoptic		BH solution		Mt-BH-LPs	
	Single	Long-term	Single	Long-term	Single	Long-term	Single	Long-term
Cornea	0	0	0	0	0	0	0	0
Iris	0	0	0	0	0	0	0	0
Conjunctival congestion	0	0.7	0.3	1	1	2	0.3	1
Conjunctival edema	0	0	0	0.3	0	0.3	0	0
Secretions	0	0	0	0	0	0	0	0
Total score	0	0.7	0.3	1.3	1	2.3	0.3	1

Abbreviations: Mt-BH-LPs, montmorillonite–betaxolol hydrochloride liposomes; BH, betaxolol hydrochloride.

These scores demonstrated that Mt-BH-LPs showed no sign of irritation effects on ocular tissues in rabbit eyes and even lower irritation than BH and commercial Betoptic.

Histological analysis of corneal sections of different formulations after long-term irritation testing is shown in Figure 12. In Figure 12A, the normal cornea shows a smooth and clear tissue structure. Satisfactory epithelium and stroma structure with a little edema was maintained after administration of normal saline (Figure 12B). However, after treatment with Betoptic, superficial epithelial cells were damaged and some gaps on the surface of the cornea observed (Figure 12C). Mild inflammation in corneal epithelial cells was observed after administration of BH (Figure 12D). Moreover, in eyes treated with Mt-BH-LPs, corneal epithelial cells exhibited some slight edema after long-term irritation tests (Figure 12E). Figure 13 presents the immunohistochemistry of conjunctiva after long-term irritation tests with different formulations. Conjunctiva treated with normal saline (Figure 13B) showed slight inflammation with a bulge on the cell surface compared with normal conjunctiva (Figure 13A). In addition, conjunctiva receiving Betoptic and BH also both showed a chronic inflammation, as verified by the appearance of some hyperemia and cellular damage (Figure 13C and D). For the Mt-BH-LP group (Figure 13E), conjunctiva revealed little infiltration of lymphocytes without obvious inflammation. Histological analysis demonstrated that corneas and conjunctiva did not show cell infiltration, hemorrhage, or necrosis after treatment with Mt-BH-LPs, indicating that Mt-BH-LPs had lower toxicity for the conjunctiva and cornea than BH solution and Betoptic after long-term irritation tests.

CAM-TBS

The Hen's egg test–CAM (HET-CAM) method was employed to study the macroscopic changes in the CAM, such

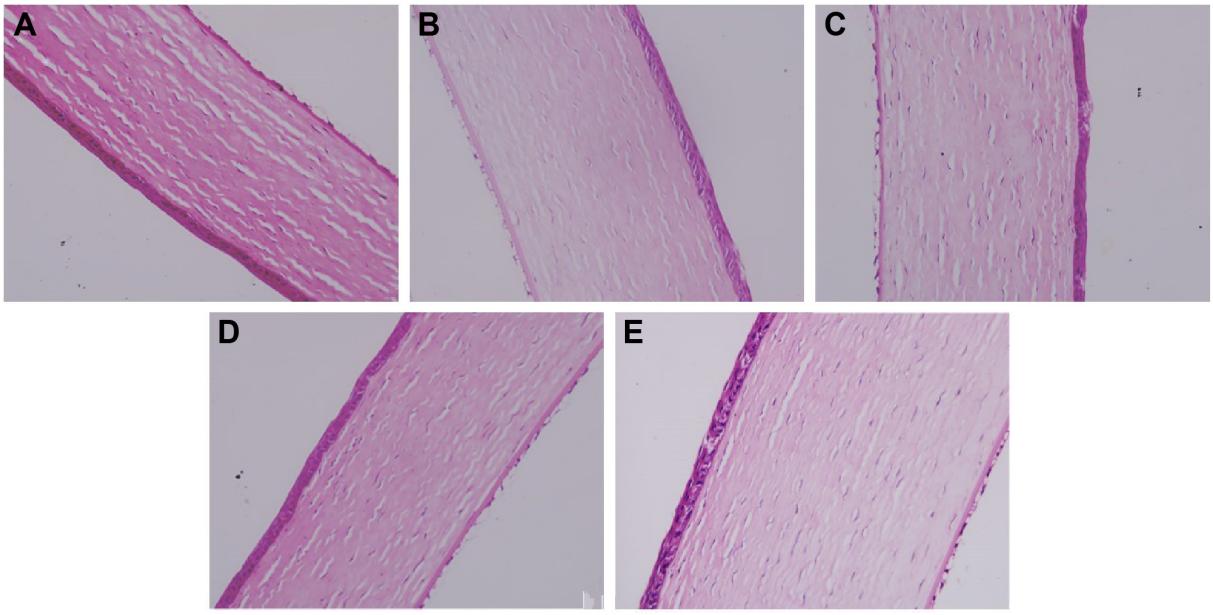

Figure 12 Cornea histopathology by microscopy.
Notes: (**A**) Normal cornea, (**B**) treated with saline, (**C**) treated with Betoptic, (**D**) treated with BH solution, and (**E**) treated with Mt-BH-LPs.
Abbreviations: Mt-BH-LPs, montmorillonite–betaxolol hydrochloride liposomes; BH, betaxolol hydrochloride.

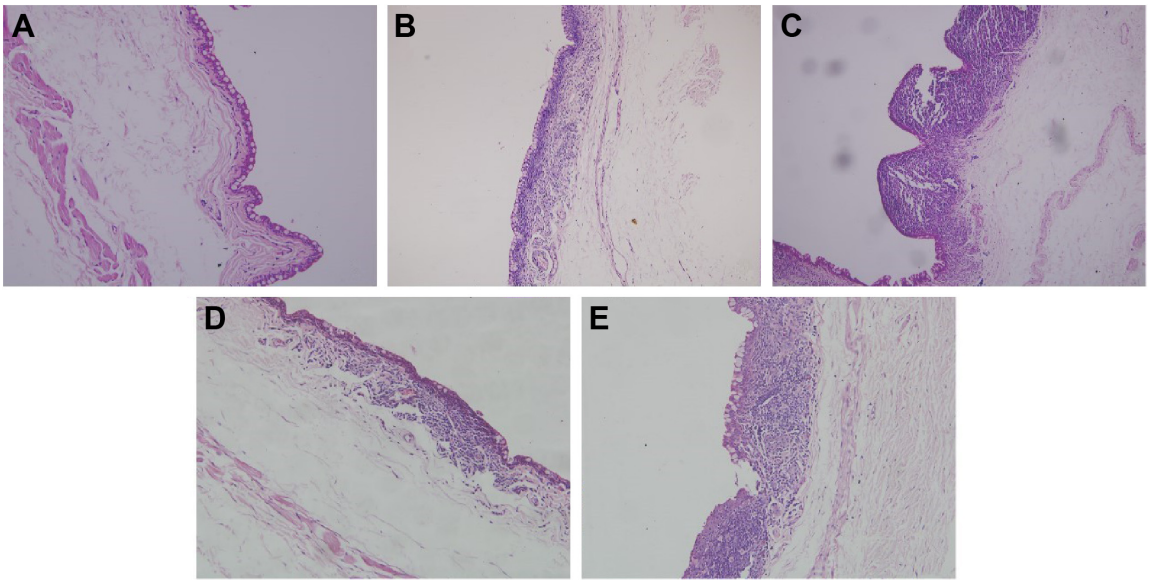

Figure 13 Conjunctival histopathology by microscopy.
Notes: (**A**) Normal cornea, (**B**) treated with saline, (**C**) treated with Betoptic, (**D**) treated with BH solution, and (**E**) treated with Mt-BH-LPs.
Abbreviations: Mt-BH-LPs, montmorillonite–betaxolol hydrochloride liposomes; BH, betaxolol hydrochloride.

as hyperemia, hemorrhage, and coagulation, following treatment with test substances (Figure 14A). Previous work has reported that the HET-CAM test is not fully representative of eye irritation.[49,50] Therefore, the CAM-TBS method was developed to offer an objective estimation strategy to overcome the disadvantages of lack of objectivity and quantitativeness resulting from the HET-CAM method.[51] This CAM-TBS method was designed to evaluate the negative effect of substances by measuring the amount of TB adsorbed with the CAM as the end point of the assay. TBS has been widely applied for measuring cell viability and detecting destruction and denaturation of the membrane. Absorption for TB was in the order of NaOH (positive control) > BH > Betoptic > Mt-BH-LPs > normal saline (NS) (negative control) (Figure 14B). These results were consistent with values estimated by the Draize test, which revealed the Mt-BH-LPs were safe for ocular drug delivery.

Precorneal retention of Mt-BH-LPs

In vitro precorneal retention of Mt-BH-LPs

Histologically, the construct appears as a stratified epithelium, and it could bear resemblance to normal human corneal epithelium (Figure 15). Cell-culture models of ocular barriers could provide powerful systems to investigate pharmacokinetic properties of Mt-BH-LPs. There is a hypothesis that human TF volume is 7 μL and the tear production rate 1.3 μL·min^{-1}, and so we scaled up these parameters by a factor of 38, putting 270 μL of STF in the turnover chamber and fixing 50 μL·min^{-1} tear flux.[52] Residence times on corneal epithelium/TF compartment after an application of Mt-BH-LPs in comparison with BH solution are shown in Figure 16. The highest BH concentration (about 38.87 μg·mL^{-1}) was observed immediately after application of BH and rapidly fell to undetectable values in less than 60 minutes. For Mt-BH-LPs, an increase in BH concentration, followed by almost a plateau and a subsequent decrease, was observed. BH concentrations reached undetectable values at more than 110 minutes. These data suggested Mt-BH-LPs maintained drug concentrations in aqueous humor for a longer time than BH.

In vivo precorneal retention of Mt-BH-LPs

Pharmacokinetic parameters (Table 2) were estimated by using a pharmacokinetic program: 3p87, produced by the Mathematics Pharmacological Committee of the Chinese Academy of Pharmacology. The half-life, mean residence time, and area under the curve of Mt-BH-LPs were 15.7, 2.6, and 4.8 times greater than those of BH solution, respectively. Figure 17 shows BH concentration in rabbit tears as a function of time. Although the general trend of the two formulations versus time curves was similar, the BH concentration of Mt-BH-LPs was higher than that of the BH solution at each time point. For the BH solution, the BH concentration in tears rapidly fell from about 400 μg·mL^{-1} at 5 minutes to 18 μg·mL^{-1} within 30 minutes. Compared with the BH solution, the BH concentrations of Mt-BH-LPs in tears were higher (about three times) than those of BH solution at the same intervals.

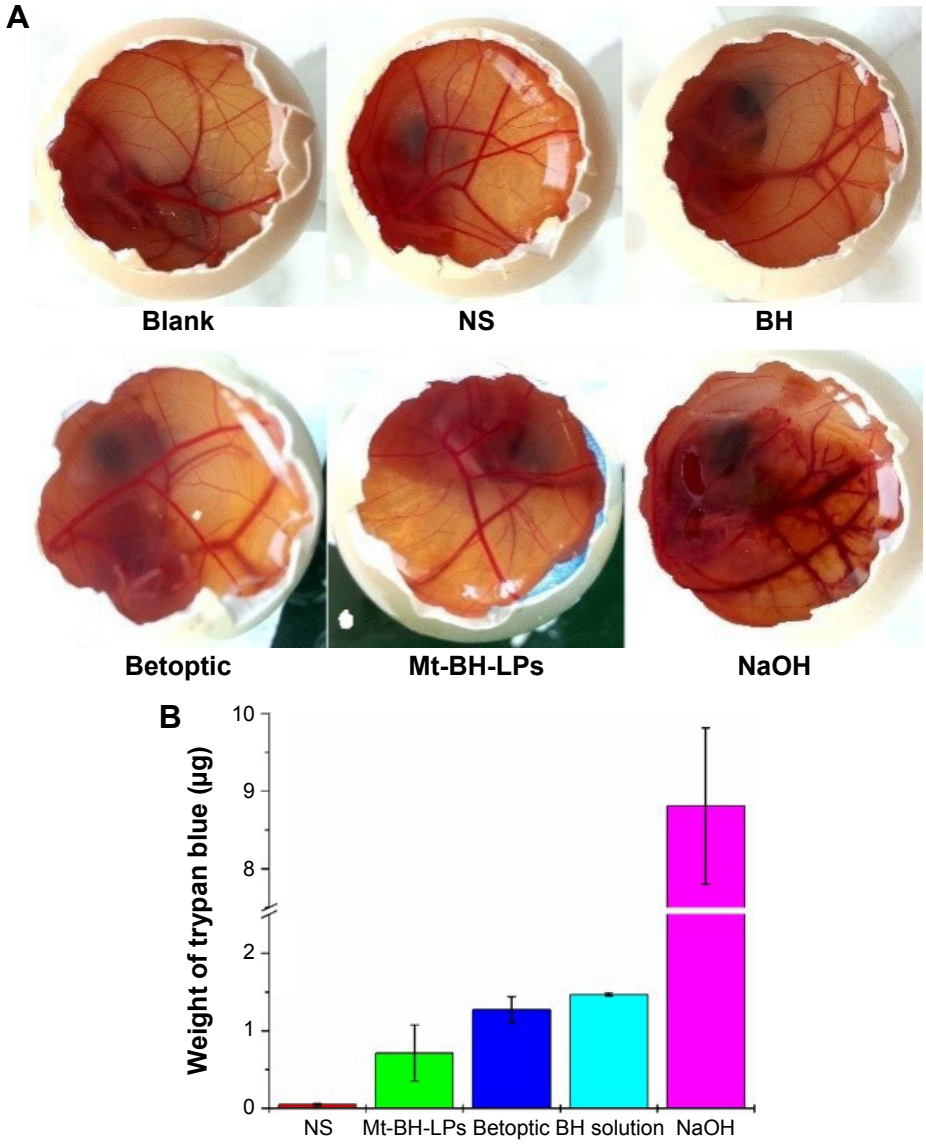

Figure 14 (**A**) Hemorrhage situation and (**B**) trypan blue absorption of CAM.
Abbreviations: NS, normal saline; Mt-BH-LPs, montmorillonite–betaxolol hydrochloride liposomes; BH, betaxolol hydrochloride; CAM, chorioallantoic membrane.

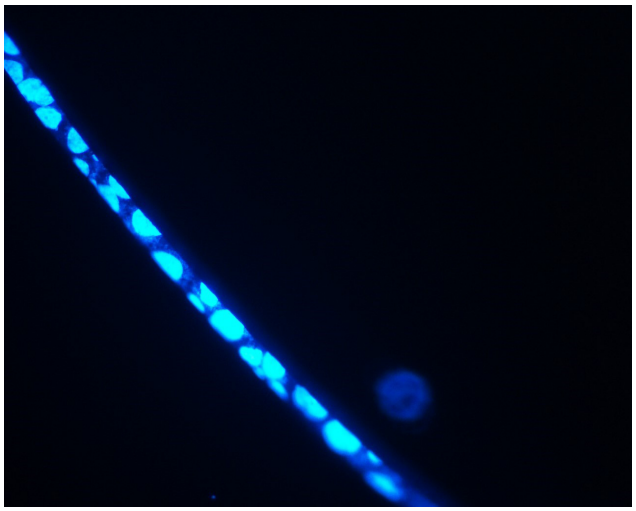

Figure 15 Frozen section of stratified immortalized human cornea epithelial cells.
Note: Fluorescence microscope image (magnification 400×).

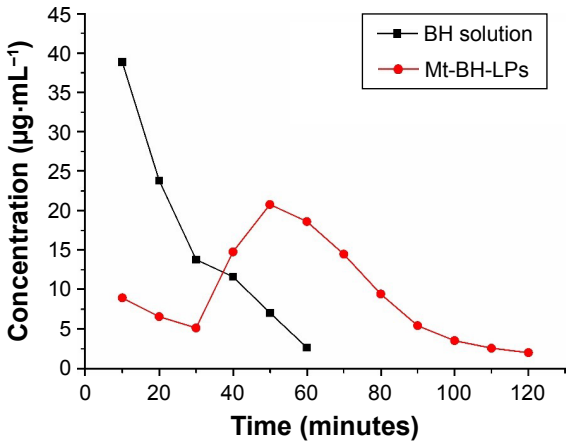

Figure 16 Concentration–time curve in the cornea/tear-film compartment after topical application of BH solution and Mt-BH-LPs.
Abbreviations: Mt-BH-LPs, montmorillonite–betaxolol hydrochloride liposomes; BH, betaxolol hydrochloride.

Table 2 Pharmacokinetics parameters of BH in tears after topical administration in rabbits

	BH solution	Mt-BH-LPs	BH/Mt-BH-LPs ratio
k (min^{-1})	0.14±0.06	0.045±0.05	0.32
$t_{1/2}$ (minutes)	5.67±2.88	89.02±39.98	15.7
MRT (minutes)	9.36±1.8	24.57±8.93	2.6
AUC_{0-t} ($\mu g \cdot min \cdot mL^{-1}$)	4,883.43±17	23,244±3,495.85	4.8

Abbreviations: Mt-BH-LPs, montmorillonite–betaxolol hydrochloride liposomes; BH, betaxolol hydrochloride; $t_{1/2}$, half-life; MRT, mean residence time; AUC, area under the curve.

Interestingly, the BH concentration of 13.6 $\mu g \cdot mL^{-1}$ in Mt-BH-LPs was detected even at 240 minutes. This indicated that Mt-BH-LPs can remain in the corneal area, which was consistent with results estimated by the in vitro pharmacokinetic studies. These results revealed that Mt-BH-LPs might prolong the retention time of the drugs on the ocular surface and slow drug elimination, thus enhancing ocular bioavailability of topically dosed ophthalmic drugs.

Pharmacodynamic studies

Figure 18 shows changes in IOP in rabbits for three groups (normal saline, BH, and Mt-BH-LPs) to determine therapeutic efficacy. In general, IOP was elevated in rabbits by placing them in a dark room.[32] IOP increased by 4–5.5 mmHg compared with untreated rabbits (15.03 mmHg) after 5 hours in the dark. This enhanced IOP was usually maintained for at least 8 hours in the dark. It can be seen from Figure 18 that both BH and Mt-BH-LPs obviously impeded the enhancement in IOP compared with normal saline. Interestingly, the reduction in IOP for Mt-BH-LPs was greater than for BH. It can be observed from the curve that the IOP of BH even significantly declined by 24% after 1 hour, but rapidly returned to baseline values after 6 hours (20.14 mmHg). Conversely, Mt-BH-LPs showed a slight decrease in IOP of 22.4% after 2 hours, and then slowly elevated to 19.45 mmHg below baseline values after 6 hours. This implied that the novel preparation of Mt-BH-LPs effectively prolonged the IOP-lowering effect after administration.

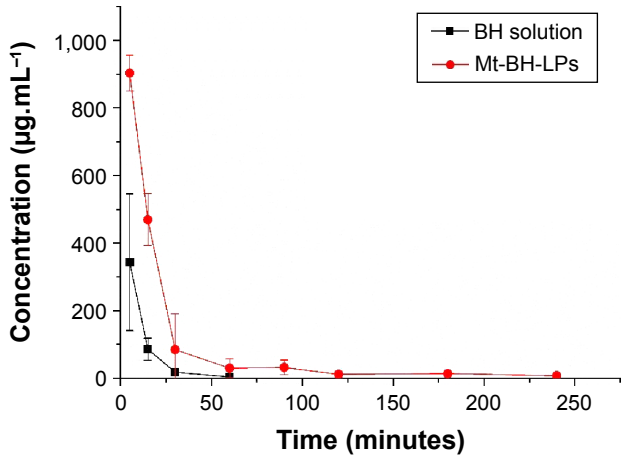

Figure 17 Mean tear-fluid concentration–time curve after topical application of BH solution and Mt-BH-LPs in rabbit eyes.
Abbreviations: Mt-BH-LPs, montmorillonite–betaxolol hydrochloride liposomes; BH, betaxolol hydrochloride.

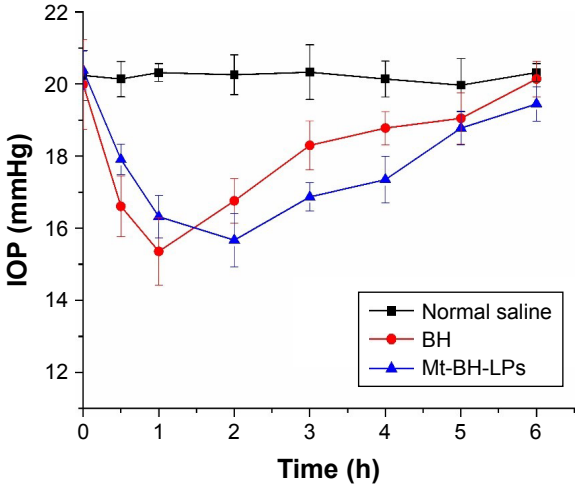

Figure 18 Change in IOP for rabbits with saline, BH solution, and Mt-BH-LPs.
Abbreviations: IOP, intraocular pressure; Mt-BH-LPs, montmorillonite–betaxolol hydrochloride liposomes; BH, betaxolol hydrochloride.

Conclusion

In summary, a novel ion-exchange drug-delivery system based on Mt-BH nanocomposite incorporated into LPs (Mt-BH-LPs) was developed. Mt-BH and Mt-BH-LPs were prepared by acidification and ethanol injection combined with an ammonium sulfate gradient. Data from TGA, XRD, FTIR, and TEM demonstrated the successful formation of the Mt-BH nanocomposite and Mt-BH-LP formulation. Mt-BH-LPs were supposed to be of small PS and exhibit sustained release, as estimated by dynamic light scattering and in vitro release, respectively. MTT, CAM-TBS, and in vivo rabbit eye-irritation tests all demonstrated that Mt-BH-LPs induced no obvious irritation and were comparatively safe for ophthalmic delivery. Both in vitro and in vivo precorneal retention of Mt-BH-LPs revealed that they might increase the precorneal residence time of BH and reduce precorneal drug loss. Therefore, Mt-BH-LPs can decrease IOP more effectively than BH solution. From the aforementioned results, Mt-BH-LPs have been demonstrated to be a potential candidate for ocular drug delivery.

Acknowledgments

This work was financially supported by the National Natural Science Foundation of China (grant 51102052) and Medical Scientific Research Foundation of Guangdong Province,

China (grant A2016275). The Eye Institute of Shandong Province is acknowledged for the provision of iHCECs. This study was approved by the Ethics Committee of Shandong Eye Institute and all experiments were carried out in accordance with the Declaration of Helsinki.

Disclosure

The authors report no conflicts of interest in this work.

References

1. Caprioli J, Coleman AL. Intraocular pressure fluctuation a risk factor for visual field progression at low intraocular pressures in the advanced glaucoma intervention study. *Ophthalmology*. 2008;115(7):1123–1129.
2. Jung HJ, Abou-Jaoude M, Carbia BE, Plummer C, Chauhan A. Glaucoma therapy by extended release of timolol from nanoparticle loaded silicone-hydrogel contact lenses. *J Control Release*. 2013;165(1):82–89.
3. Gallarate M, Chirio D, Bussano R, et al. Development of O/W nanoemulsions for ophthalmic administration of timolol. *Int J Pharm*. 2013;440(2):126–134.
4. Huang W, Zhang N, Hua H, et al. Preparation, pharmacokinetics and pharmacodynamics of ophthalmic thermosensitive in situ hydrogel of betaxolol hydrochloride. *Biomed Pharmacother*. 2016;83:107–113.
5. Davies NM. Biopharmaceutical considerations in topical ocular drug delivery. *Clin Exp Pharmacol Physiol*. 2000;27(7):558–562.
6. Dai Y, Zhou R, Liu L, Lu Y, Qi J, Wu W. Liposomes containing bile salts as novel ocular delivery systems for tacrolimus (FK506): in vitro characterization and improved corneal permeation. *Int J Nanomedicine*. 2013;8:1921–1933.
7. Chetoni P, Monti D, Tampucci S, et al. Liposomes as a potential ocular delivery system of distamycin A. *Int J Pharm*. 2015;492(1–2):120–126.
8. Zhang J, Liang X, Li X, et al. Ocular delivery of cyanidin-3-glycoside in liposomes and its prevention of selenite-induced oxidative stress. *Drug Dev Ind Pharm*. 2016;42(4):546–553.
9. Aksungur P, Demirbilek M, Denkbaş EB, Vandervoort J, Ludwig A, Unlü N. Development and characterization of cyclosporine A loaded nanoparticles for ocular drug delivery: cellular toxicity, uptake, and kinetic studies. *J Control Release*. 2011;151(3):286–294.
10. Duxfield L, Sultana R, Wang R, et al. Development of gatifloxacin-loaded cationic polymeric nanoparticles for ocular drug delivery. *Pharm Dev Tech*. 2015;21(2):172–179.
11. Andrés-Guerrero V, Zong M, Ramsay E, et al. Novel biodegradable polyesteramide microspheres for controlled drug delivery in ophthalmology. *J Control Release*. 2015;211:105–117.
12. Osswald CR, Kang-Mieler JJ. Controlled and extended release of a model protein from a microsphere-hydrogel drug delivery system. *Ann Biomed Eng*. 2015;43(11):2609–2617.
13. Hippalgaonkar K, Adelli GR, Hippalgaonkar K, Repka MA, Majumdar S. Indomethacin-loaded solid lipid nanoparticles for ocular delivery: development, characterization, and in vitro evaluation. *J Ocul Pharmacol Ther*. 2013;29(2):216–228.
14. Leonardi A, Bucolo C, Drago F, Salomone S, Pignatello R. Cationic solid lipid nanoparticles enhance ocular hypotensive effect of melatonin in rabbit. *Int J Pharm*. 2015;478(1):180–186.
15. Horvát G, Gyarmati B, Berkó S, et al. Thiolated poly(aspartic acid) as potential in situ gelling, ocular mucoadhesive drug delivery system. *Eur J Pharm Sci*. 2015;67:1–11.
16. Wu Y, Yao J, Zhou J, Dahmani FZ. Enhanced and sustained topical ocular delivery of cyclosporine A in thermosensitive hyaluronic acid-based in situ forming microgels. *Int J Nanomedicine*. 2013;8:3587–3601.
17. Maulvi FA, Lakdawala DH, Shaikh AA, et al. In vitro and in vivo evaluation of novel implantation technology in hydrogel contact lenses for controlled drug delivery. *J Control Release*. 2016;226:47–56.
18. Lajunen T, Hisazumi K, Kanazawa T, et al. Topical drug delivery to retinal pigment epithelium with microfluidizer produced small liposomes. *Eur J Pharm Sci*. 2014;62:23–32.
19. Shafaa MW, Sabra NM, Fouad RA. The extended ocular hypotensive effect of positive liposomal cholesterol bound timolol maleate in glaucomatous rabbits. *Biopharm Drug Dispos*. 2011;32(9):507–517.
20. Asasutjarit R, Theerachayanan T, Kewsuwan P, Veeranodha S, Fuongfuchat A, Ritthidej GC. Development and evaluation of diclofenac sodium loaded-N-trimethyl chitosan nanoparticles for ophthalmic use. *AAPS Pharm Sci Tech*. 2015;16(5):1013–1024.
21. Aguzzi C, Cerezo P, Viseras C, Caramella C. Use of clays as drug delivery systems: possibilities and limitations. *Appl Clay Sci*. 2007;36(1–3):22–36.
22. Hou DZ, Hu S, Huang Y, et al. Preparation and in vitro study of lipid nanoparticles encapsulating drug loaded montmorillonite for ocular delivery. *Appl Clay Sci*. 2016;119(2):277–283.
23. Zheng JP, Luan L, Wang HY, Xi LF, Yao KD. Study on ibuprofen/montmorillonite intercalation composites as drug release system. *Appl Clay Sci*. 2007;36(4):297–301.
24. Fejér I, Kata M, Erös I, Berkesi O, Dékány I. Release of cationic drugs from loaded clay minerals. *Colloid Polym Sci*. 2001;279(12):1177–1182.
25. Nunes CD, Vaz PD, Fernandes AC, Ferreira P, Romão CC, Calhorda MJ. Loading and delivery of sertraline using inorganic micro and mesoporous materials. *Eur J Pharm Biopharm*. 2007;66(3):357–365.
26. Hou DZ, Gui RY, Hu S, Huang Y, Zuyong Feng ZY, Ping QN. Preparation and characterization of novel drug-inserted-montmorillonite chitosan carriers for ocular drug delivery. *Adv Nanopart*. 2015;4(3):70–84.
27. Kevadiya BD, Joshi GV, Mody HM, Bajaj HC. Biopolymer-clay hydrogel composites as drug carrier: host-guest intercalation and in vitro release study of lidocaine hydrochloride. *Appl Clay Sci*. 2011;52(4):364–367.
28. Joshi GV, Kevadiya BD, Patel HA, Bajaj HC, Jasra RV. Montmorillonite as a drug delivery system: intercalation and in vitro release of timolol maleate. *Int J Pharm*. 2009;374(1–2):53–57.
29. Gandhi R, Khatri N, Baradia D, Vhora I, Misra A. Surface-modified epirubicin-HCl liposomes and its in vitro assessment in breast cancer cell-line: MCF-7. *Drug Deliv*. 2016;23(4):1152–1162.
30. Yu Y, Lu Y, Bo R, et al. The preparation of gypenosides liposomes and its effects on the peritoneal macrophages function in vitro. *Int J Pharm*. 2014;460(1–2):248–254.
31. Vega E, Egea MA, Calpena AC, et al. Role of hydroxypropyl-β-cyclodextrin on freeze-dried and gamma-irradiated PLGA and PLGA-PEG diblock copolymer nanospheres for ophthalmic flurbiprofen delivery. *Int J Nanomedicine*. 2012;7:1357–1371.
32. Gokce EH, Sandri G, Bonferoni MC, et al. Cyclosporine A loaded SLNs: evaluation of cellular uptake and corneal cytotoxicity. *Int J Pharm*. 2008;364(1):76–86.
33. Buda I, Budai P, Szabó R, Lehel J. In vitro eye corrosion study of agrochemicals on isolated chicken eye. *Commun Agric Appl Biol Sci*. 2013;78(2):177–181.
34. Li J, Liu H, Liu LL, Cai CN, Xin HX, Liu W. Design and evaluation of a brinzolamide drug-resin in situ thermosensitive gelling system for sustained ophthalmic drug delivery. *Chem Pharm Bull (Tokyo)*. 2014;62(10):1000–1008.
35. Nagai N, Yoshioka C, Mano Y, et al. A nanoparticle formulation of disulfiram prolongs corneal residence time of the drug and reduces intraocular pressure. *Exp Eye Res*. 2015;132:115–123.
36. Zhang W, Li X, Ye T, et al. Design, characterization, and in vitro cellular inhibition and uptake of optimized genistein-loaded NLC for the prevention of posterior capsular opacification using response surface methodology. *Int J Pharm*. 2013;454(1):354–366.
37. Joshi GV, Kevadiya BD, Bajaj HC. Controlled release formulation of ranitidine-containing montmorillonite and Eudragit E-100. *Drug Dev Ind Pharm*. 2010;36(9):1046–1053.

38. Chiu CW, Chu CC, Cheng WT, Lin JJ. Exfoliation of smectite clays by branched polyamines consisting of multiple ionic sites. *Eur Polym J*. 2008;44(3):628–636.
39. Kevadiya BD, Thumbar RP, Rajput MM, et al. Montmorillonite/poly-(ε-caprolactone) composites as versatile layered material: reservoirs for anticancer drug and controlled release property. *Eur J Pharm Sci*. 2012;47(1):265–272.
40. Kevadiya BD, Patel TA, Jhala DD, et al. Layered inorganic nanocomposites: a promising carrier for 5-fluorouracil (5-FU). *Eur J Pharm Biopharm*. 2012;81(1):91–101.
41. Kevadiya BD, Chettiar SS, Rajkumar S, Bajaj HC, Gosai KA, Brahmbhatt H. Evaluation of clay/poly (l-lactide) microcomposites as anticancer drug, 6-mercaptopurine reservoir through in vitro cytotoxicity, oxidative stress markers and in vivo pharmacokinetics. *Colloids Surf B Biointerfaces*. 2013;112:400–407.
42. Tsai CC, Juang TY, Dai SA, et al. Synthesis and montmorillonite-intercalated behavior of dendritic surfactants. *J Mater Chem*. 2006; 16(21):2056–2063.
43. Li SL, Jiang CX, Chen XM, Wang H, Lin J. *Lactobacillus casei* immobilized onto montmorillonite: survivability in simulated gastrointestinal conditions, refrigeration and yogurt. *Food Res Int*. 2014;64:822–830.
44. Kevadiya BD, Joshi GV, Patel HA, Ingole PG, Mody HM, Bajaj HC. Montmorillonite-alginate nanocomposites as a drug delivery system: intercalation and in vitro release of vitamin B1 and vitamin B6. *J Biomater Appl*. 2010;25(2):161–177.
45. Kevadiya BD, Joshi GV, Bajaj HC. Layered bionanocomposites as carrier for procainamide. *Int J Pharm*. 2010;388(1–2):280–286.
46. Iliescu RI, Andronescu E, Ghitulica CD, Voicu G, Ficai A, Hoteteu M. Montmorillonite-alginate nanocomposite as a drug delivery system: incorporation and in vitro release of irinotecan. *Int J Pharm*. 2014; 463(2):184–192.
47. Kevadiya BD, Rajkumar S, Bajaj HC, et al. Biodegradable gelatin-ciprofloxacin-montmorillonite composite hydrogels for controlled drug release and wound dressing application. *Colloids Surf B Biointerfaces*. 2014;122:175–183.
48. Kaunisto E, Tajarobi F, Abrahmsen-Alami S, Larsson A, Nilsson B, Axelsson A. Mechanistic modelling of drug release from a polymer matrix using magnetic resonance microimaging. *Eur J Pharm Sci*. 2013; 48(4–5):698–708.
49. Lawrence RS, Ackroyd DM, Williams DL. The chorioallantoic membrane in the prediction of eye irritation potential. *Toxicol In Vitro*. 1990;4(6): 321–323.
50. Reinhardt CA, Pelli DA, Zbinden G. Interpretation of cell toxicity data for the estimation of potential irritation. *Food Chem Toxicol*. 1985;23(2): 247–252.
51. Hagino S, Itagaki H, Kato S, Kobayashi T. Further evaluation of the quantitative chorioallantoic membrane test using trypan blue stain to predict the eye irritancy of chemicals. *Toxicol In Vitro*. 1993;7(1): 35–39.
52. Giannola LI, de Caro V, Giandalia G, Siragusa MG, Cordone L. Ocular gelling microspheres: in vitro precorneal retention time and drug permeation through reconstituted corneal epithelium. *J Ocul Pharmacol Ther*. 2008;24(2):186–196.